



## METHODS OF PROTECTING RAILWAY TRANSPORT FROM WIND

**Bozorov R.Sh.<sup>1</sup><sup>a</sup>, Boboev D.Sh.<sup>1</sup><sup>d</sup>,**

<sup>1</sup>*Tashkent state transport university, Tashkent, Uzbekistan*

**Abstract:** *Currently, one of the pressing issues in railway transport is the problem of soil movement in windy areas, especially in desert areas. It is important to study the negative effects of wind on railway infrastructure and provide scientifically based solutions in this area. For this purpose, the effects of wind on the stability of rolling stock were studied.*

**Keywords:** *Freight and passenger trains, empty containers, wind gusts, wind speed, aerodynamic pressure, sand drift, obstacles.*

Even if the container was tightly fastened to Rama, with the repeated danger of rama and the container capsizing through skolzun, the dissertation looked at traditional methods of protecting rail transport from the wind. The main ways to protect rail transport from the wind are as follows.

- Construction of railway Woodlands;
- Construction of engineering structures and protective screens along the railway;
- Change and strengthen the structural features of bridge transfers;
- Increase the stability of the moving content and change the constructive features.

Rail protective woodlands can perform several tasks at once [1-5].

- prevent the formation of snow drifts;
- weakening wind power to moving content;
- helps prevent soil decay and soil erosion;
- reduces noise levels in rail transport.

In order to reduce the wind, seedlings with a dense structure of three rows are planted.

In relation to the railway, shrubs are planted in the first nearest row, the next two rows are planted alternately with the main trees and tree species that are related to it (Figure 1) [12-15].

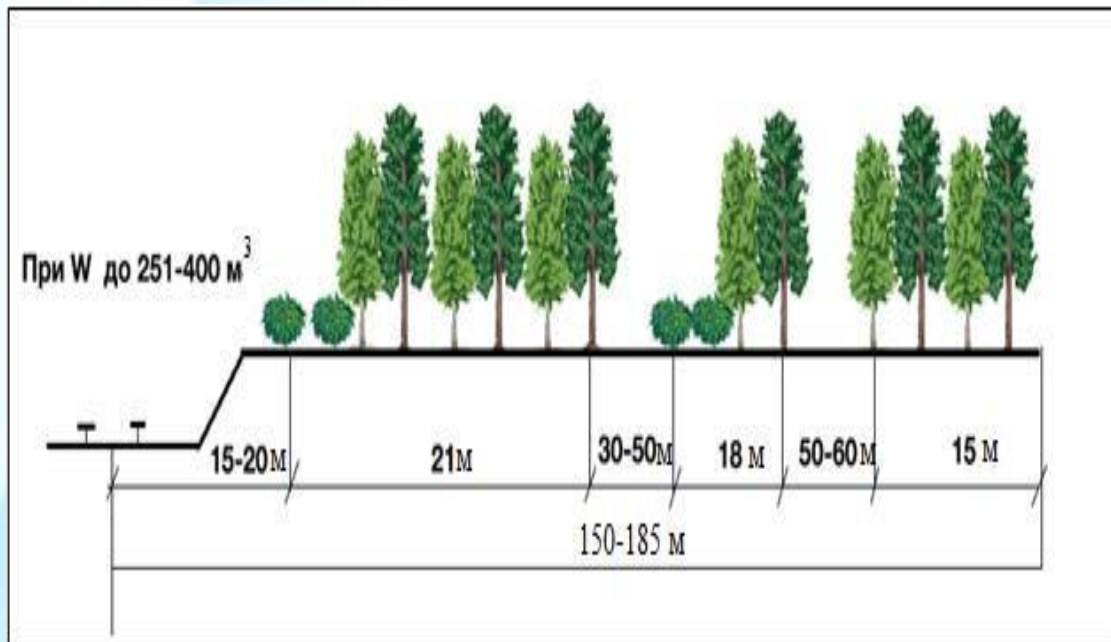


*Figure 1. Scheme of a wind-damping, snow-protecting forest line along the railways*

In rail transport, shielding is one of the methods of wind attenuation. As a rule, screens are covered to reduce noise in rail transport. In wind attenuation, however, the shielding method is not economically desirable, so perforated barriers made of steel profile panels are used [6-8].

Perforated barriers are installed along the tracks to prevent sand from slipping on the tracks. They prevent the sand from passing onto the track and ensure that trains can move safely. In addition, the screens protect the railway from the entry of alien individuals and wildlife, as well as provide stable movement of the train, acting as a barrier from the wind in areas with mutually strong winds. Wind protection screens can be used effectively where crops cannot be planted due to lack of water and poor soil conditions. The perforated steel wall controls and changes the direction of wind currents, reduces wind speed, reduces the strength and volume of vortex currents, and prevents dust from spreading. When using a steel panel structure, the holes allow the



wind to pass through the wall and reduce its speed, so the wind will not have lifting power [9-10, 16-20].

Wind protection screen functions:

- reducing wind power;
- air flow control;
- dust dispersion;
- sudden wind protection;
- reducing the strength of crosswinds;
- optimal air circulation;
- protection against wild animals;
- protection from strangers.

These steel panel systems are characterized by low cost, wide application, and ease of installation. (Figure 2) shows examples of wind fencing.



*Figure 2. Examples of installation of wind barriers*

The wind protection barrier consists of a metal load-bearing frame and perforated profile panels. The panels (a perforated shaped layer) are attached to a metal frame mounted on the foundation using a bolt connection. The carcass is made of two layers of balms, shvellers, corner-shaped metals. Windproof perforated panels are made of zinc-treated steel with a thickness of 1 to 1.5 mm. For additional protection

against corrosion, the panels are covered with polymer powder paint [12-15].

In the practice of bridge construction, there have been several cases of collapse of bridge structures under the influence of wind forces.

Failure to take wind power into account resulted in the collapse of the Tay Rail Bridge rail bridge (1979), the collapse of the Tacoma-Narrows Bridge in Washington state (1940), the collapse of the right - of-way on the Obskaya-Bovanenko highway in Yamal (2008) -, an incomplete list of accidents caused by excessive dynamic twisting vibrations caused by wind. .

To prevent negative aerodynamic phenomena of the Kerch Bridge, aerodynamic covers of the “Aircraft Wing” were developed. These structures reduce the wind impact in the cupric range [21-24].

Such measures are a passive way to combat vibrations.



*Figure 3. Aerodynamic device of the Crimean Bridge.*

A distinctive feature of the aerodynamic device is the ease of their installation and use. Modeling results obtained using Solidworks Flow simulation and ANSYS FLUENT package applications.

In the modeling process, the conditions for ensuring the stability of the cargo being transported in the structure of open movement and the analysis of “Wind Flower” in the cross-section of the regions on the scale of the injection MTU UK were taken into account.



Develop 3D models of open Motion Content, which were generated directly using Compass-3D and Solidworks package programs (figures 4-6).

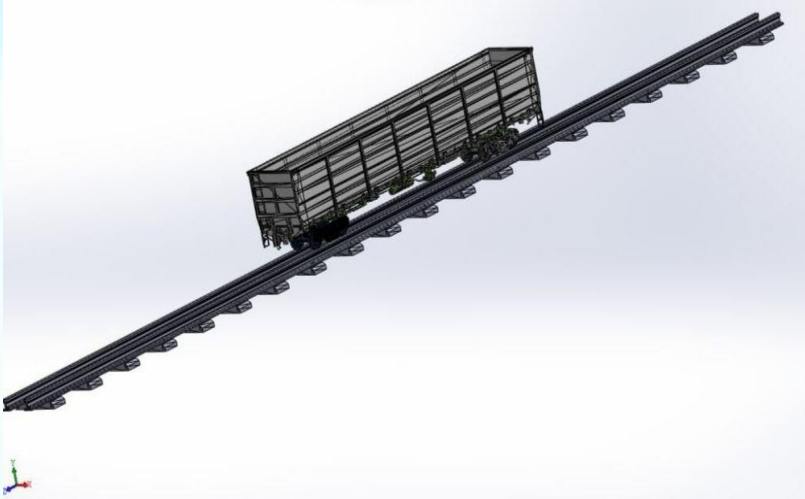


*Figure 4. The Compass is a 3D model of semi-open wagons using 3D package software.*

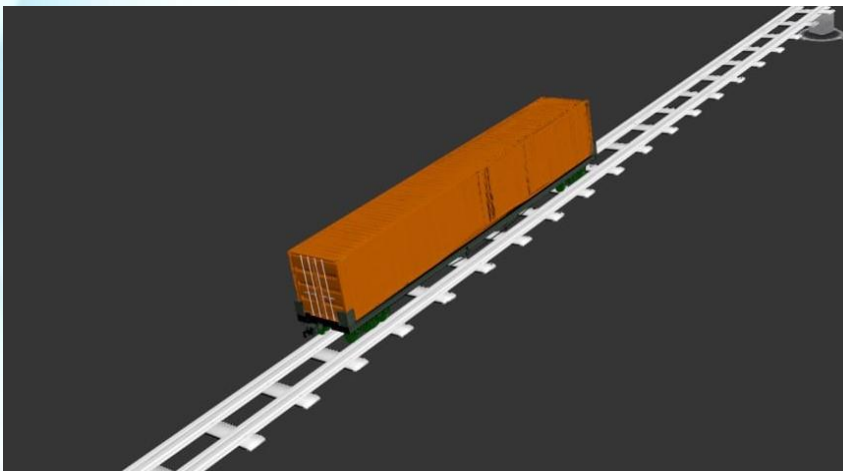


*Figure 5. Compass is a container 3D model placed on a platform using 3D package software.*

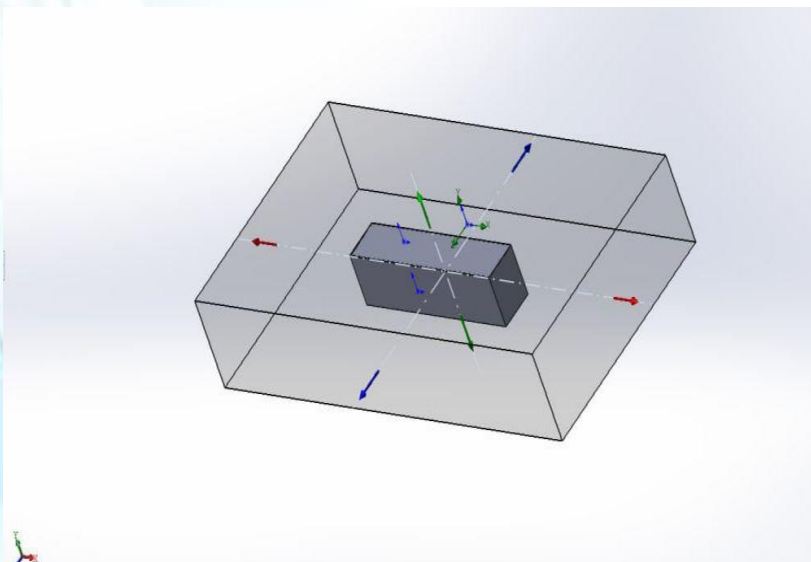


Figure 6. 3D model of a 40-foot universal container obtained using Solidworks package software.

The accounting work focused on ensuring the stagnation of 40-foot universal empty containers. To this end, taking into account the complex conditions of the stagnation of the universal container, the greatest aerodynamic effect of the wind on them from the transverse direction was modeled. This used the SolidWorks Flow simulation package software.

Considering the peak pressure effects, an external wind speed of 30 M/s (108 km / h) was adopted. In the process of calculation results and modeling, the following graphs were formed (figures 7-10).

Список целей

Имя	Текущее значение	Прогресс сходимости	Критерий	Среднее значение
GG Максимум Полное давление 3	102016 Pa	Достигнуто (IT = 62)	14.7665 Pa	102016 Pa
GG Максимум Скорость (X) 6	18.3102 m/s	Достигнуто (IT = 95)	0.0534063 m/s	18.3207 m/s
GG Максимум Скорость (Y) 9	25.8325 m/s	Достигнуто (IT = 89)	0.0982479 m/s	25.8598 m/s
GG Максимум Скорость (Z) 12	21.5523 m/s	Достигнуто (IT = 105)	1.46841 m/s	20.2131 m/s
GG Минимум Полное давление 1	100798 Pa	Достигнуто (IT = 62)	41.1841 Pa	100806 Pa
GG Минимум Скорость (X) 4	-18.3389 m/s	Достигнуто (IT = 108)	0.0541188 m/s	-18.3496 m/s
GG Минимум Скорость (Y) 7	-22.7659 m/s	Достигнуто (IT = 62)	0.197649 m/s	-22.7682 m/s
GG Минимум Скорость (Z) 10	-31.5817 m/s	Достигнуто (IT = 83)	0.398405 m/s	-31.5953 m/s
GG Момент (X) 18	-93145.8 N*m	Достигнуто (IT = 78)	2211.08 N*m	-93085.9 N*m
GG Момент (Y) 19	130458 N*m	Достигнуто (IT = 58)	3846.11 N*m	130584 N*m
GG Момент (Z) 20	2057.29 N*m	Достигнуто (IT = 82)	1302.88 N*m	2001.2 N*m
GG Сила (X) 16	-26.3048 N	16%	1.71654 N	-25.6248 N
GG Сила (Y) 17	244.254 N	Достигнуто (IT = 82)	181.129 N	241.839 N
GG Сила по нормали (X) 13	-26.4128 N	16%	1.71543 N	-25.7482 N
GG Сила по нормали (Y) 14	243.962 N	Достигнуто (IT = 82)	181 N	241.253 N
GG Сила по нормали (Z) 15	-18178.7 N	Достигнуто (IT = 58)	527.39 N	-18167 N
GG Среднее Полное давление 2	101747 Pa	Достигнуто (IT = 66)	3.04698 Pa	101748 Pa
GG Среднее Скорость (X) 5	0.00709938 m/s	13%	0.000360256 m/s	0.0043234 m/s
GG Среднее Скорость (Y) 8	-0.149793 m/s	Достигнуто (IT = 87)	0.0527721 m/s	-0.138217 m/s
GG Среднее Скорость (Z) 11	-25.3246 m/s	Достигнуто (IT = 66)	0.183761 m/s	-25.3333 m/s

Figure 7. Calculation results of external wind influences on the universal container, which is fastened to a special platform.

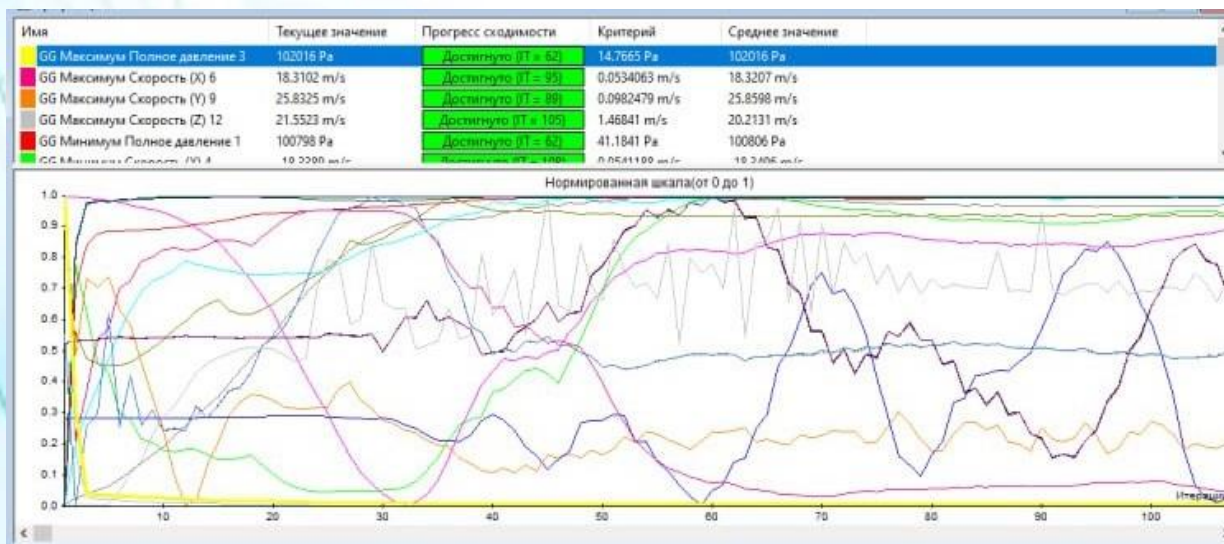


Figure 8. Calculation result graphs on the Axes X, Y, Z of airflow, aerodynamic pressure, rotating moments.

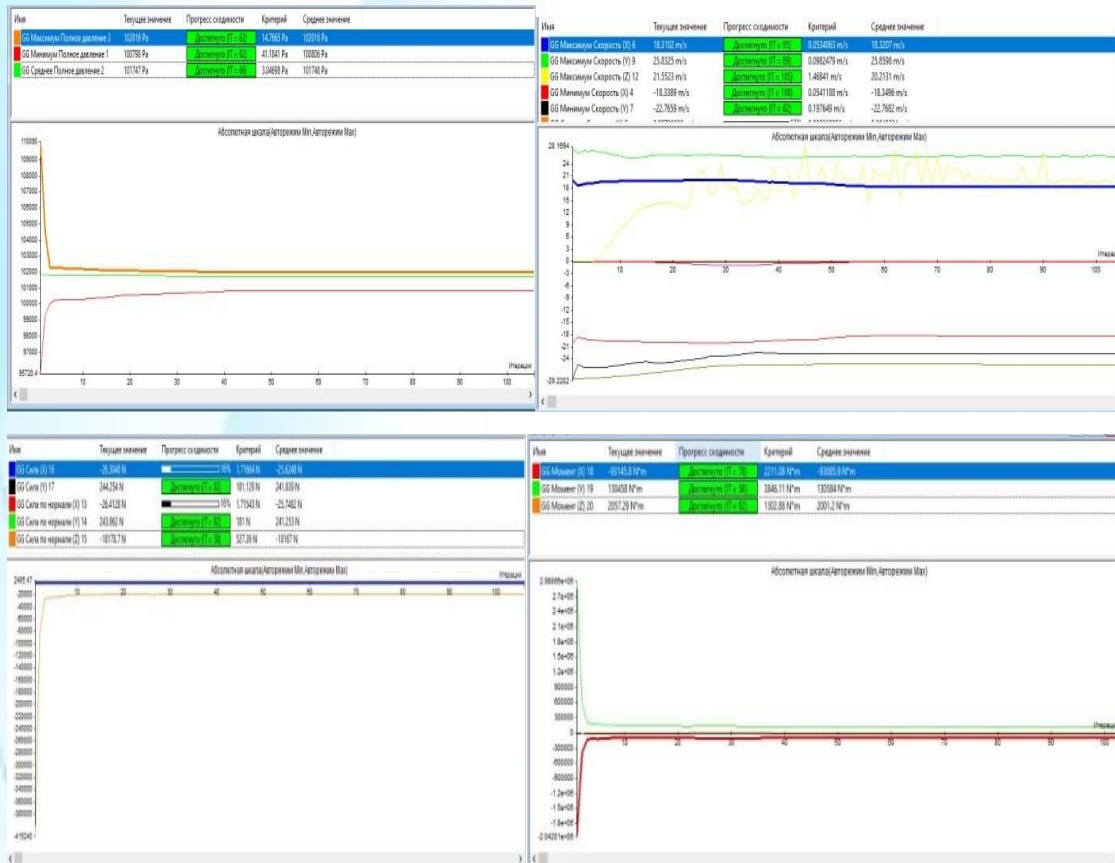
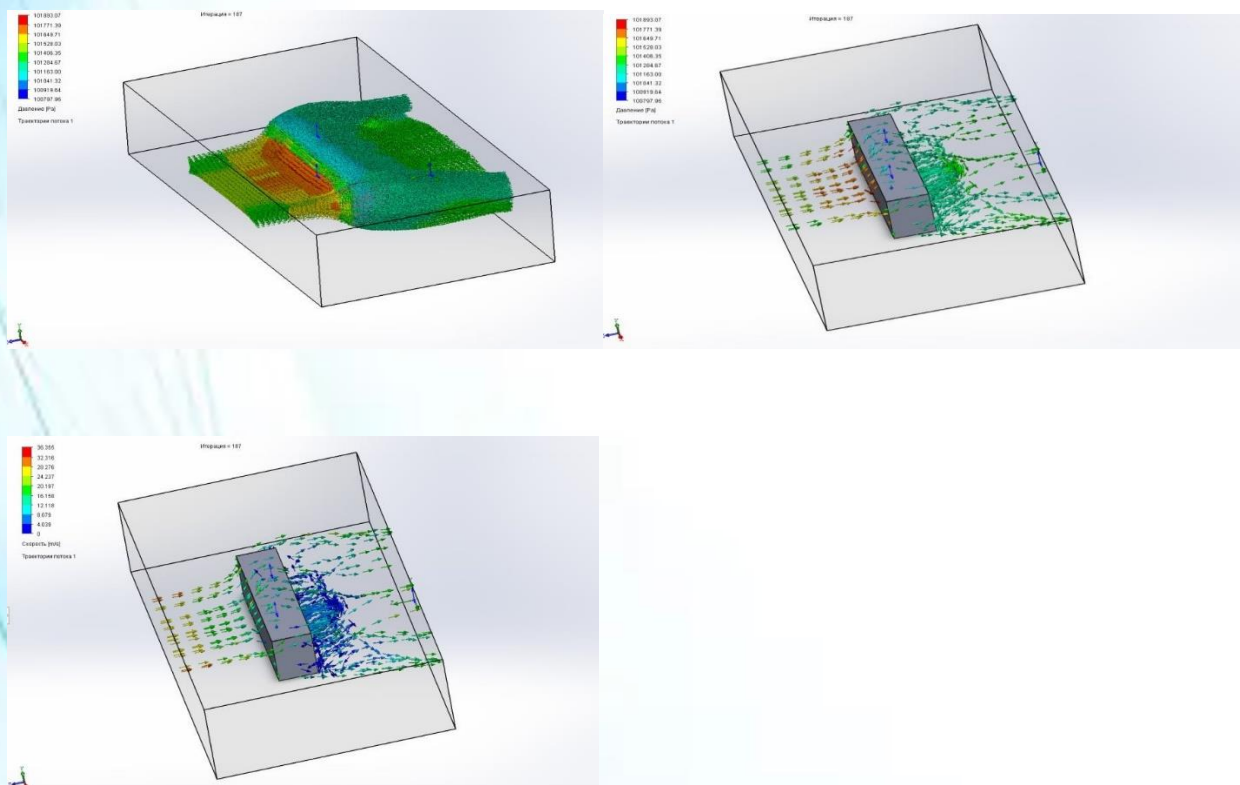


Figure 9. Dynamics of calculation change of maximum and minimum pressure, air flow rate and normal forces.





*Figure 10. The result of the air flow (wind) velocity vector model acting in the transverse direction.*

The results of the calculation showed that the maximum pressure exerted on the wagon body is 102,016 KPa, as well as the amount of torque exerted on the lunar route is 130,458 KN\*m, which in turn requires head containers to be fastened with additional fastening equipment in these areas.

### **REFERENCES**

1. Bozorov R. Sh. Aerodynamic impact of the high-speed electric train «Afrosiyob» on opposite trains. Journal of Transsib Railway Studies, 2022, no. 2 (50), pp. 96-107 (In Russian).
2. Bozorov R.S., Rasulov M.X., Masharipov M.N. Investigation of mutual aerodynamic influence of high-speed passenger and freight trains moving on adjacent tracks. Journal Innотrans Scientific-and-nonfiction edition, 2022, no. 2(44), pp. 42-48. DOI:10.20291/2311-164X-2022-2-42-48
3. “EN 14067 Railway applications – Aerodynamics – Part 2: Aerodynamics on open track”, ed: CEN/TC 256, 2010.
4. “EN 14067 Railway applications – Aerodynamics – Part 4: Requirements and test procedures for aerodynamics on open track”, ed: CEN/TC 256, 2010.
5. Lazarenko Y.M., Kapuskin A.N. Aerodynamic impact of the «Sapsan» high-speed electric train on passengers on platforms and on oncoming trains when crossing. Bulletin of the Research Institute of Railway Transport, 2012, no. 4, pp.11-14 (In Russian).
6. Raghu S. Raghunathan, H. D. Kim, T. Setoguchi. Aerodynamics of high-speed railway train / Progress in Aerospace Sciences 38 (2002) 469-514.
7. Baker C., Quinn A., Sima M., Hoefener L., and Licciardello R. Full-scale measurement and analysis of train slipstreams and wakes. Part 1: Ensemble averages. Proceedings of the Institute of mechanical Engineers, Part F: Journal of Rail and Rapid Transit, 2013. p. 453-467.
8. Baker C., Quinn A., Sima M., Hoefener L., and Licciardello R. Full scale measurement and analysis of train slipstreams and wakes: Part 2 Gust analysis.





Proceedings of the Institute of mechanical Engineers, Part F: Journal of Rail and Rapid Transit, 2013. p. 468-480.

9. Katsuyuki M., Kazuaki I., Tsutomu H., Jin'ichi O., Kei H. and Atsuyushi H. Effect of train draft on platforms and in station houses. JR East Technical Review No. 16, 2010. p. 39-42.

10. Hong Wu, Zhi-jian Zhou. Study on aerodynamic characteristics and running safety of two high-speed trains passing each other under crosswinds based on computer simulation technologies. Journal of Vibroengineering, Vol. 19, Issue 8, 2017, p. 6328-6345.

11. Tian Li , Ming Li, Zheng Wang and Jiye Zhang. Effect of the inter-car gap length on the aerodynamic characteristics of a high-speed train. Journal of Rail and Rapid transit, Issue 4, September 20, 2018, p. 448-465.

12. Chris Baker, Terry Johnson, Dominic Flynn, Hassan Hemida, Andrew Quinn, David Soper, Mark Sterling. Train Aerodynamics fundamentals and applications. Book Butterworth-Heinemann London 2019, p. 151-179. ISBN 978-0-12-813310-1, <https://doi.org/10.1016/B978-0-12-813310-1.00008-3>

13. Bozorov R.Sh., Rasulov M.Kh., Bekzhanova S.E., Masharipov M.N. Methods for the efficient use of the capacity of sections in the conditions of the passage of high-speed passenger trains. Journal Railway transport: Topical issues and innovations, 2021, no. 2, pp. 5-22. (In Russian).

14. Shukhrat Saidivaliev, Ramazon Bozorov, Elbek Shermatov. Kinematic characteristics of the car movement from the top to the calculation point of the marshalling hump. E3S Web of Conferences 264, 05008 (2021) <https://doi.org/10.1051/e3sconf/202126405008>

15. Rasulov, M., Masharipov, M., Sattorov, S., & Bozorov, R. (2023). Study of specific aspects of calculating the throughput of freight trains on two-track railway sections with mixed traffic. In E3S Web of Conferences (Vol. 458, p. 03015). EDP Sciences. <https://doi.org/10.1051/e3sconf/202345803015>

16. Bozorov R.Sh. About absence of theoretical base of the formula for determination of height of the first profile site of the marshalling hump / Bozorov R.Sh., Saidivaliev



- Sh.U., Djabbarov Sh.B. –Text : immediate // Innovation. The science. Education. 2021, №34. pp. 1467–1481. (In Russian).
17. Bozorov R. S., Rasulov M. X., Masharipov M. N. Research on the aerodynamics of high-speed trains // Universum: технические науки: электрон. научн. журн., 2022, № 6 (99).
18. Marufdjan Rasulov, Masud Masharipov, S. E. Bekzhanova and Ramazon Bozorov. Measures of effective use of the capacity of twotrack sections of JSC “Uzbekistan Railways”. E3S Web of Conferences 401, 05041 (2023) <https://doi.org/10.1051/e3sconf/202340105041>
19. Andrzej Zbieć. Aerodynamic Phenomena Caused by the Passage of a Train. Part 2: Pressure Influence on Passing Trains. Problemy Kolejnictwa. Issue 192, September 2021, p. 195-202. <http://dx.doi.org/10.36137/1926E>
20. NB JT ST 03-98. Safety standards for railway transport. Electric trains. – M.: VNIIT, 2003. – 196 p.
21. UIC 566 Leaflet: Loadings of coach bodies and their components, 3<sup>rd</sup> edition of 1.1.90
22. Saidivaliev, Sh.U. A new method of calculating time and speed of a carriage during its movement on the section of the first brake position of a marshaling hump when exposed headwind / Sh.U. Saidivaliev, R.Sh. Bozorov, E.S. Shermatov // STUDENT eISSN: 2658-4964. 2021, №9.
23. Bozorov R.Sh., Saidivaliev Sh.U., Shermatov E.S., and Boboev D.Sh. Research to establish the optimal number of platforms in a container. Transport: science, technology, management. Scientific information collection. Issue 5, 2022, p. 24-28. <https://doi.org/10.36535/0236-1914-2022-05-5> (In Russian).
24. Rasulov, M., Masharipov, M., & Ismatullaev, A. (2021). Optimization of the terminal operating mode during the formation of a container block train. In *E3S Web of Conferences* (Vol. 264, p. 05025). EDP Sciences. <https://doi.org/10.1051/e3sconf/202126405025>